IN-92
114129
P.23

NASA Technical Memorandum 105827

Photovoltaic Array for Martian Surface Power

J. Appelbaum
National Aeronautics and Space Administration
Lewis Research Center
Cleveland, Ohio

and

G.A. Landis
Sverdrup Technology, Inc.
Lewis Research Center Group
Brook Park, Ohio

Prepared for the
43rd Congress of the International Astronautical Federation
sponsored by the AIAA, NASA, and NAS
Washington, D.C., August 28—September 5, 1992

(NASA-TM-105827) PHOTOVOLTAIC ARRAY FOR MARTIAN SURFACE POWER (NASA) 23 p

N92-33899

Unclas

G3/92 0114129

NASA

PHOTOVOLTAIC ARRAYS FOR MARTIAN SURFACE POWER

Joseph Appelbaum[1] and Geoffrey A. Landis[2]

NASA Lewis Research Center 302-1
Cleveland, OH 44135 U.S.A.

Abstract

Missions to Mars will require electric power. A leading candidate for providing power is solar power provided by photovoltaic arrays. To design such a power system, detailed information on solar radiation availability on the Martian surface is necessary. The variation of the solar radiation on the Martian surface is governed by three factors: (1) variation in Mars-Sun distance, (2) variation in solar zenith angle due to Martian season and time of day, and (3) dust in the Martian atmosphere. A major concern is the dust storms, which occur on both local and global scales. However, there is still appreciable diffuse sunlight available even at high opacity, so that solar array operation is still possible. Typical results for tracking solar collectors are also shown and compared to the fixed collectors. During the northern hemisphere spring and summer the insolation is relatively high, 2-5 kW-hr/m^2-day, due to the low optical depth of the Martian atmosphere. These seasons, totalling a full terrestrial year, are the likely ones during which manned missions will be carried out.

1 Introduction

Missions to the Martian surface and activities there will require electric power. Unmanned survey missions may require power levels ranging from hundreds of watts to a few kilowatts; a manned Mars base would be likely to require tens to hundreds of kilowatts; while a facility to process in-situ resources such as rocket propellants could require power on the order of megawatts. A leading candidate for providing this power is solar power produced by photovoltaic arrays. To design such a power system, detailed information on solar radiation availability on the Martian surface is necessary.

Mars is a challenging environment for the use of solar power. The twelve-hour night, although not as severe as the moon's 14 day darkness, still requires that any solar power system include a large storage system. Mars is further from the sun, and thus the solar intensity in Mars orbit is less than half that at Earth (the eccentricity of the orbit means that the actual intensity varies by $\pm 19\%$ during the year). Furthermore, the atmosphere is filled with dust. Even on clear days the sky is partialy obscured with atmospheric dust, and during dust storms the atmosphere becomes nearly opaque.

---

[1] Tel-Aviv University, Faculty of Engineering, Ramat-Aviv 69978, Israel. NRC Resident Research Associate at NASA Lewis Research Center, Cleveland, OH 44135, USA.

[2] Sverdrup Technology, Inc., Brook Park, OH 44142, USA.

Solar irradiance at the surface of Mars varies with season and with the amount of atmospheric dust [1]. A major concern is the dust storms, which occur on both local and global scales, and their effect on solar array output. Global storms occur near the perihelion, and may persist for long periods of time, such that the requirement for energy storage quickly becomes much too large to be practical. However, as we have shown [2, 3], there is still an appreciable diffuse component of sunlight available even at high opacity (optical depth), so that some solar array output will still be possible.

From a photovoltaic system design point of view, the intensity, frequency, and duration of these storms may be viewed as "partially cloudy" and "cloudy" days for which additional energy storage must be taken into account.

The full sky, or "global," solar radiation is composed of a direct (unscattered, or "beam") component, and a diffuse (scattered by the atmosphere) component. Given the optical depth of the atmosphere [4], the global radiation is calculated from the normalized net solar flux function based on calculated multiple scattering of the incident radiation integrated over multiple incident wavelengths [5]. The direct beam component is derived from the optical depth of the atmosphere using Beer's law, and the diffuse component is the difference of the global and direct radiation.

2 Optical Depth

For our purposes, the intensity of the dust storms on Mars can be defined in terms of the resulting opacity of the Martian atmosphere. This is most conveniently measured in terms of the optical depth τ, defined as the logarithm of the attenuation of the direct component of a beam penetrating the atmosphere perpendicular to the surface. An optical depth of 1 corresponds to attenuation of the beam by a factor of e.

The most direct and probably most reliable estimates of opacity are those derived from Viking Lander imaging of the Sun. Figs. 1 and 2 show the seasonal variation of the normal incidence of the optical depth at the Viking Lander locations VL1 and VL2, respectively. The season is indicated by position of Mars in its orbit around the sun, measured by the areocentric longitude of the Sun L_s, where at the Mars vernal equinox $L_s = 0°$.

The measurements are at the sites of the two Viking landers. Viking Lander 1 (VL1) is located at 22.3° N latitude and 47.9° W longitude, and Viking Lander 2 (VL2) is located at 47.7° N latitude and 225.7° W longitude. Figs. 1 and 2, derived from ref. [4] and discretized for each 5°, show the optical depth at the two sites. The optical depth is assumed to remain constant throughout the day. Opacities are minimum during the northern spring (L_s = 0° to 90°) and summer (L_s = 90° to 180°), and maximum during southern spring (L_s = 180° to 270°) and summer (L_s = 270° to 360°), the seasons during which most local and major dust storms occur. When dust storms are not present, the optical depth is typically about 0.5. Two global dust storms occurred during the periods of each observation, as indicated by the high values of the optical depth. These values are lower bound values; the actual optical depth may be higher. The two global dust storms that were observed by the Viking Landers make 1977 one of the worst years of dust activities on Mars observed. It should be noted, however, that there may be some Mars years which have no global dust storms [1].

3 Solar Radiation

3.1 Radiation at the Top of the Mars Atmosphere

The variation of the solar radiation at the top of the Mars atmosphere is governed by the location of Mars in its orbit and by the solar zenith angle. The solar radiation is entirely direct beam radiation. The beam irradiance, in W/m^2, is given by [1,2]:

$$G_{ob} = 590\frac{[1 + e\cos(L_s - 248)]^2}{(1 - e^2)^2} \tag{1}$$

where e = 0.093377 is the eccentricity of the orbit of Mars, L_s is the areocentric longitude, and 248° is the areocentric longitude of Mars perihelion. (Here we use the subscript 'o' for air mass zero, indicating intensity above the atmosphere, and the subscript b to indicate the direct (beam) component). This irradiance is shown in Fig. 3.

3.2 Solar Radiation on the Surface of Mars

The variation of the solar radiation on the Martian surface is governed by three factors: (1) the Mars-Sun distance, which varies the intensity at the top of the atmosphere, as discussed in the previous section, (2) the solar zenith angle, z, and (3) the opacity of the Martian atmosphere. The global solar irradiance G is the sum of the direct beam irradiance G_b, the diffuse irradiance G_d, and the irradiance due to albedo G_{al} (i.e., light reflected to the array from the surface):

$$G = G_b + G_d + G_{al} \tag{2}$$

The direct beam irradiance on the Martian surface normal to the solar rays is related by Beer's law to the optical depth, τ, of the intervening atmospheric haze:

$$G_b = G_{ob}\exp[-\tau/\cos z] \tag{3}$$

where z is the sun zenith angle.

3.2.1 Horizontal surface

The beam irradiance on a horizontal surface is given by:

$$G_{bh} = G_{ob}\cos z\exp(-\tau/\cos z) \tag{4}$$

For a horizontal surface $G_{al} = 0$, and the global irradiance G_h is:

$$G_h = G_{ob}\cos z\frac{f(z,\tau,al)}{(1 - al)} \tag{5}$$

where al is the albedo. $f(z,\tau,al)$ is called the normalized net solar flux function and accounts for the light which penetrates the atmospheric dust. The net solar flux integrated over the solar

spectrum on the Martian surface was calculated by Pollack [5] based on multiple wavelength and multiple scattering of the solar radiation. Derived data from this calculation can be approximated by a polynomial expression:

$$f(z,\tau,al) = \left[\sum_{i=0}^{5}\sum_{j=0}^{5}\sum_{k=0}^{1} p(i,j,k)\cdot\tau^i\cdot\left(\frac{z}{100}\right)^j\cdot(al)^k\right](1-al) \tag{6}$$

where p(i,j,k) are the coefficients of the polynomial given in Table I. The diffuse irradiance is obtained by subtracting the beam irradiance from the global irradiance (eqs. (4) and (5)).

The daily global insolation (integrated solar energy per unit area) on a horizontal surface is obtained by integrating the irradiance over the period from sunrise to sunset:

$$H_h = \frac{24.65^\star}{2\pi} G_{ob}\int_{\omega_{sr}}^{\omega_{ss}} \cos z\,\frac{f(z,\tau,al)}{(1-al)}\,d\omega \tag{7}$$

where ω_{sr} and ω_{ss} are the sunrise and sunset hour angles, respectively. The daily beam insolation on a horizontal surface is obtained by:

$$H_{bh} = \frac{24.65^\star}{2\pi}\int_{\omega_{sr}}^{\omega_{ss}} \cos z\exp(-\tau/\cos z)\,d\omega \tag{8}$$

and the daily diffuse insolation on a horizontal surface H_{dh} is the difference between the global and the beam insolations.

Solar radiation data is given for the locations of Viking Landers VL1 and VL2 based on the measured optical depths by the Viking Lander cameras. Solar radiation data at other latitudes are discussed in [3] and will be also presented elsewhere. The daily global insolation in kW-hr/m^2-day on a horizontal surface on Mars at VL1 and VL2 is shown in Fig. 4. The daily global insolation at VL1 and VL2 is repeated again in Figs. 5 (a) and (b) but together with the percentage of the diffuse insolation H_{dh}/H_h. The figure shows that during spring and summer where the optical depth is relatively low, the diffuse insolation comprises about 50 percent of the global insolation, whereas for autumn and winter, the optical depth is high and therefore the diffuse insolation comprises about 90 percent.

As mentioned before, there may be years on Mars which have no global storms (clear skies). The optical depth of the atmosphere for clear skies is typically 0.5. It is interesting to compare the insolation on the surface of Mars for clear skies with that for the opacities observed in 1977 by Viking [2,3]. This comparison is shown in Fig. 6. As one can see, the effect of the global storms is more pronounced at the lower latitude site VL1 than at the higher latitude site VL2.

---

* These equations are in terms of actual (terrestrial) hours. A Martian day is 24.65 terrestrial hours long. In some cases it is convenient to define a "Mars hour" to be 1/24th of the Martian day, or 2.7% longer than a terrestrial hour. To get the insolation on Mars with reference to these Mars hours, replace the 24.65 in the numerator by 24 hr.

3.2.2 Inclined Surface

The solar radiation on an inclined surface is based on solar radiation data on an horizontal surface G_h and G_{dh}. The global irradiance G_β on an inclined surface with an angle β is given by:

$$G_\beta = G_b \cos\theta + G_{dh} \cos^2(\beta/2) + al\ G_h \sin^2(\beta/2) \tag{9}$$

where G_b is given in eq. (3) and θ is the angle of incidence, the angle between the beam direction and the normal to the surface. The insolation on the surface is obtained by integrating the irradiance over the period from sunrise to sunset. The integration may be replaced by a summation, obtaining:

$$H_\beta = \sum_{\omega_{cr}}^{\omega_{cs}} G_{bi} \cos\theta_i \Delta\omega + \sum_{\omega_{sr}}^{\omega_{ss}} [G_{dhi} \cos^2(\beta/2) + alG_{hi} \sin^2(\beta/2)]\Delta\omega \tag{10}$$

where the subscript i corresponds to the irradiance at solar angle w_i and $\Delta\omega$ is the solar angle interval.

For collecting direct irradiance, the daily optimum tilt angle β for a south-facing surface in the northern hemisphere is:

$$\beta = \phi - \delta \tag{11}$$

where ϕ is the local latitude and δ the angle of the sun from the Mars equator, which varies from +25° to -25° with the season, and β=0 corresponds to a horizontal surface. Averaged over a year, the theoretical optimal inclination angle for an array surface facing south is for the tilt to be equal to the latitude:

$$\beta = \phi \tag{12}$$

The variation of the daily global insolation H_β for a surface with $\beta = \phi$ at VL1 and VL2 is shown in Fig. 7. The difference in the daily insolation for a horizontal surface and for the inclined surface with $\beta = \phi$ is shown in Fig. 8 as a percentage loss (or gain) compared to the horizontal surface. It is interesting to note that this tilt angle results in a decrease in the total yearly insolation, rather than a gain. One can observe that there is a loss in the insolation during the summer, when the optimum daily tilt angle (equation 11) is closer to horizontal than the $\beta = \phi$ yearly optimum. While a surface tilted at the latitude angle is optimum for collection of the beam radiation, it is less efficient than a horizontal surface in collecting the indirect radiation. This decreases the performance of a tilted surface in winter and fall, when indirect radiation is the largest component of the insolation received. As a result, the advantage of a tilted surface is decreased considerably in all seasons by enough that it does not outperform the horizontal surface. The yearly loss of the insolation is small: about 2 percent at VL1 and about 1.5 percent at VL2.

The insolation on an inclined surface $\beta = \phi$ for a Martian year with no global storms may be of interest. This is shown in Fig. 9 at VL1 and VL2 for a constant optical depth of $\tau = 0.5$ throughout the year.

3.2.3 Sun-tracking Surface

Lastly, we calculate the insolation for a two-axis sun-tracking surface and compare the gain in insolation to horizontal and inclined surfaces. The global irradiance on a two-axis tracking surface is given by:

$$G_{2x} = G_b + G_{dh}\cos^2(z/2) + al\ G_h \sin^2(z/2) \tag{13}$$

and the daily insolation is obtained by integration or summation of the irradiance over the period from sunrise to sunset.

The insolation on a two-axis tracking surface at VL1 and VL2 for a Martian year is shown in Fig. 10 for the observed opacities at VL1 and VL2, and in Fig. 11 for clear skies with $\tau = 0.5$. We also compared in Fig. 12 the daily global insolation on (1) a horizontal surface, (2) a fixed inclination surface with $\beta = \phi$ and (3) a two-axis tracking surface for the observed opacities at VL1 and VL2.

The two-axis tracking surface results in a gain in total insolation received at both sites. The gain is +7 percent (compared to a horizontal surface) at the VL1 site, and +20.7 percent at the VL2 site.

During the northern hemisphere spring and summer the insolation is relatively high, 2-5 kW-hr/m^2-day, due to the low optical depth of the Martian atmosphere. These seasons, totalling a full terrestrial year, are the likely ones during which manned missions will be carried out. During the northern hemisphere autumn and winter, when dust storms typically take place, the insolation is considerably lower.

4 Mars Environmental Considerations for Power Systems

Other environmental factors of importance to photovoltaic system operation on the Mars surface are the temperature and the wind. The Martian surface temperature varies from a minimum of 130° K, to as high as 300° K, with a mean of 215° K [6,7]. Air temperatures were measured by Viking at a height of 1.6 meters above the surface over a (Martian) year of measurement, including both local and global dust storms. Peak daytime temperatures varied from about 170° K at the VL2 site during a global storm, to almost 250° K near the summer solstice. Photovoltaic cell performance increases with decreasing temperatures, with peak efficiency occuring at 150-200° K; at lower temperatures the efficiency decreases. The temperature coefficient of efficiency depends on the material, and in general increases as the material bandgap decreases. Thus, low bandgap materials such as silicon and $CuInSe_2$, which have high coefficients, increase in performance rapidly at the low temperatures to be found at Mars.

Wind was also measured by Viking. The average wind speed measured at the VL2 site was about 2 m/sec [6], with winds of over 17 m/sec observed less than 1% of the time. On the average, the winds on Mars are not very high, and the extremely thin atmosphere of Mars means that the wind force is low. Abrasion by wind-blown dust of the same approximate composition as found on Mars has been measured on typical solar cell coverglass. Only wind velocities over 89 m/sec, higher than that measured by Viking, left abrasion on the coverglasses [7]. This finding is corroborated by the relative lack of abrasion damage on the Viking lander optical elements.

A final aspect of the Mars environment not well characterized is the soil. One interpretation of the Viking lander life science experiments is that the Martian soil contains large amounts of peroxides and superoxides [6]. This hypothesis needs to be confirmed by direct chemical analysis of the soil. If it is confirmed, it will be important that solar arrays be built using materials not subject to attack by oxidants.

There are several approaches to Mars photovoltaic power systems [9]. The first use will be to power unmanned rovers and scouting missions needed to investigate the geology (or areology) of Mars and scout out a location for the manned Mars base. For manned missions, the most important

criterion for a power system will be high reliability and absence of dangerous failure modes. Solar cell types to be considered include silicon, GaAs, and thin-film cells. Due to the high price of transporting materials to Mars, another priority for a surface power system is low weight. One way of reducing the weight of a photovoltaic array for Mars is to use extremely high efficiency solar cells, such as gallium-arsenide based tandem cells currently under development, with efficiency of 30% or higher. An alternative approach is to use thin-film solar cells, also now being researched. Thin-film cells have much lower efficiencies, but could be deposited in layers only a micron or two thick onto a lightweight plastic film which could be rolled out on the ground. Concentration systems, which can only take useful advantage of the direct component of the solar isolation, are less desirable on Mars, where direct insolation is only a fraction of the total energy.

Like Earth, the duration of the night on Mars varies from winter to summer depending on the latitude. This is discussed further in [9]. An energy storage system is required for operation during the night, and in some cases storage may be desirable for continuous operation during local dust storms. An example power system including a storage system for night power is discussed by McKissock, Kohout and Schmitz [10]. Their power cycle was to provide 40 kW continuous power during the day, and a reduced power level of 20 kW during the night. For the night storage capability, they assumed that the hydrogen/oxygen regenerative fuel cell (RFC) has been developed to technology readiness. The RFC assumed pressurized gas storage. Cryogenic storage of reactants was determined to require too much equipment overhead to justify the slight advantages in storage volume. Round-trip efficiency for the storage system was 61.5%.

Some resource processing technologies require thermal processing. One method of achieving high temperatures is the "solar furnace," using concentrating mirrors or lenses. Since a solar furnace, like a concentrator PV system, only utilizes the direct beam component of the solar insolation, the low direct beam insolation on Mars makes the utility of this approach much lower than in other environments.

5 Conclusions

The paper discusses solar radiation data on the surface of Mars from measurements made of the optical depths of the atmosphere at Viking Lander locations VL1 and VL2.

The two global dust storms that were observed on Mars in 1977 makes it one of the worst years of dust activities. Even so, the opacities are relatively low during the northern spring and summer for more than a half Martian year (or more than a terrestrial year) for which the insolation is relatively high, varying from about 2 to 4 kW-hr/m^2-day on a horizontal surface, and varying from about 2.5 to 5.5 kW-hr/m^2-day on a two-axis tracking surface. These seasons are the likely ones during which manned missions may be carried out.

The Martian atmosphere contains suspended dust particles, resulting in significant scattering of light. This yields a large diffuse component of the solar insolation. This is presented in Fig. 5. The diffuse insolation comprises about 50 percent of the global insolation during spring and summer and about 90 percent during autumn and winter. The effect of global dust storms on the insolation is shown in Fig. 6 where a substantial decrease in insolation is seen at VL1. The expected tilt at the yearly optimal angle $\beta = \phi$ reduces, rather than increases, the insolation on the surface during spring and summer. The insolation during autumn and winter is affected by the high opacity rather than by the inclination of the surface. For a two-axis tracking surface, the gain in insolation is about 7 percent at VL1, and about 20 percent at VL2, compared to a horizontal surface. As mentioned before, the optical depth during the global dust storms dictates the amount of insolation on a surface independently of its inclination.

6 Acknowledgements

Work at Tel Aviv University was supported under NASA grant NAGW-2022. Work done at Sverdrup Technology was supported under Contract NAS3-25266. We would also like to acknowledge the help from James B. Pollack from the Space Science Division at NASA Ames Research Center for providing the calculations of normalized net solar flux function, and for informative discussions.

References

[1] R. Haberle *et al.*, "Atmospheric Effects on the Utility of Solar Power on Mars," *Resources of Near Earth Space*, U. Arizona Press Space Science Series (in press).

[2] J. Appelbaum and D. Flood, "Solar Radiation on Mars," *Solar Energy, Vol. 45*, No. 6, pp. 353-363 (1990).

[3] J. Appelbaum and G.A. Landis, "Solar Radiation on Mars - Update 1991," NASA TM-105286 (1991); to be published in *Solar Energy*.

[4] D.S. Colburn, J.B. Pollack, and R.M. Haberle, "Diurnal Variation in Optical Depth at Mars," *Icarus, Vol. 79*, pp. 159-189 (1989).

[5] J.B. Pollack, *et al.*, "Simulation of the General Circulation of Martian Atmosphere I: Polar Processes," *J. Geophys. Res., Vol. 95*, No. B2, pp. 1447-1473 (1990).

[6] D. Kaplan, "Environment of Mars 1988," NASA Technical Memorandum 100470 (1988).

[7] J.R. Gaier, and M.E. Perez-Davis, "Effect of Particle Size of Martian Dust on the Degradation of Photovoltaic Cell Performance," NASA Technical Memorandum 105232 (1992).

[8] G.A. Landis and J. Appelbaum, "Design Considerations for Mars Photovoltaic Power Systems," *Proc. 21st IEEE Photovoltaic Specialists Conference, Vol. 2*, (IEEE, NY), pp. 1263-1270 (1990).

[9] G.A. Landis and J. Appelbaum, "Photovoltaic Power Options for Mars," *Space Power, Vol. 10*, No. 2, pp. 225-237 (1991).

[10] B. I. McKissock, L.L. Kohout and P.C. Schmitz, "A Solar Power System for an Early Mars Expedition," NASA Technical Memorandum 103219, Aug. 1990.

TABLE I – NORMALIZED NET FLUX FUNCTION COEFFICIENTS $\rho(i,j,k)$

k = 0						
j \ i	0	1	2	3	4	5
0	1.002800	-0.228681	0.019613	0.000231	-0.000130	0.000003
1	-.450073	1.335955	-1.131691	.402126	-.063967	.003758
2	5.566705	-16.912405	13.739701	-4.756079	.743740	-.043159
3	-22.471579	64.909973	-52.509470	17.997548	-2.786548	.160340
4	36.334497	-101.800319	79.895539	-26.762885	4.074117	-.231476
5	-20.420490	53.207148	-39.949537	12.977108	-1.931169	.107837
k = 1						
j \ i	0	1	2	3	4	5
0	0.009814	0.226139	-0.117733	0.030579	-0.004090	0.000218
1	-.156701	.396821	-.313648	.099227	-.013508	.000651
2	1.361122	-3.758111	3.007907	-.987457	.141693	-.007320
3	-4.365924	12.539251	-10.394165	3.486452	-.513123	.027401
4	5.991693	-17.498138	14.291370	-4.765323	.703675	-.037960
5	-2.915099	8.275686	-6.593125	2.173999	-.320308	.017335

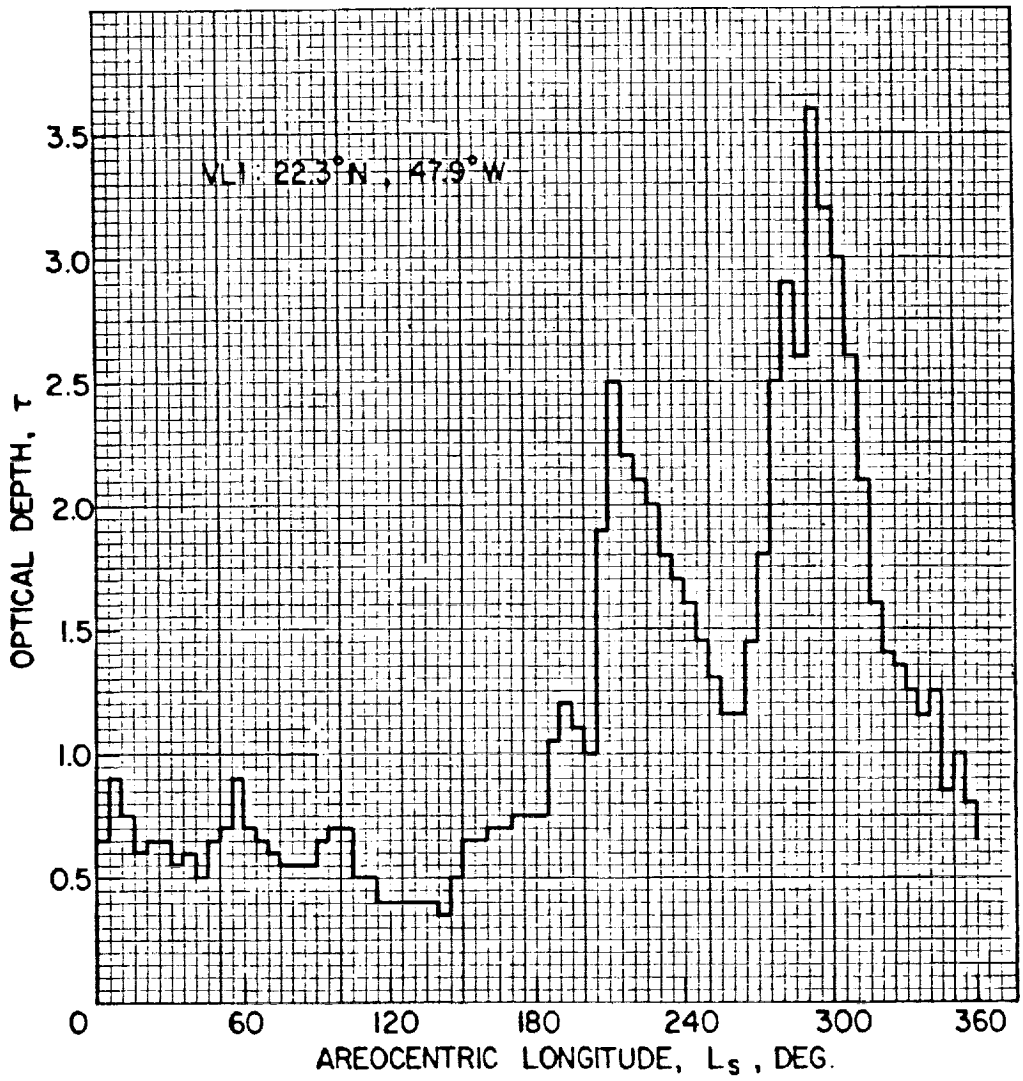

Fig. 1: Optical depth at Viking Lander VL1.

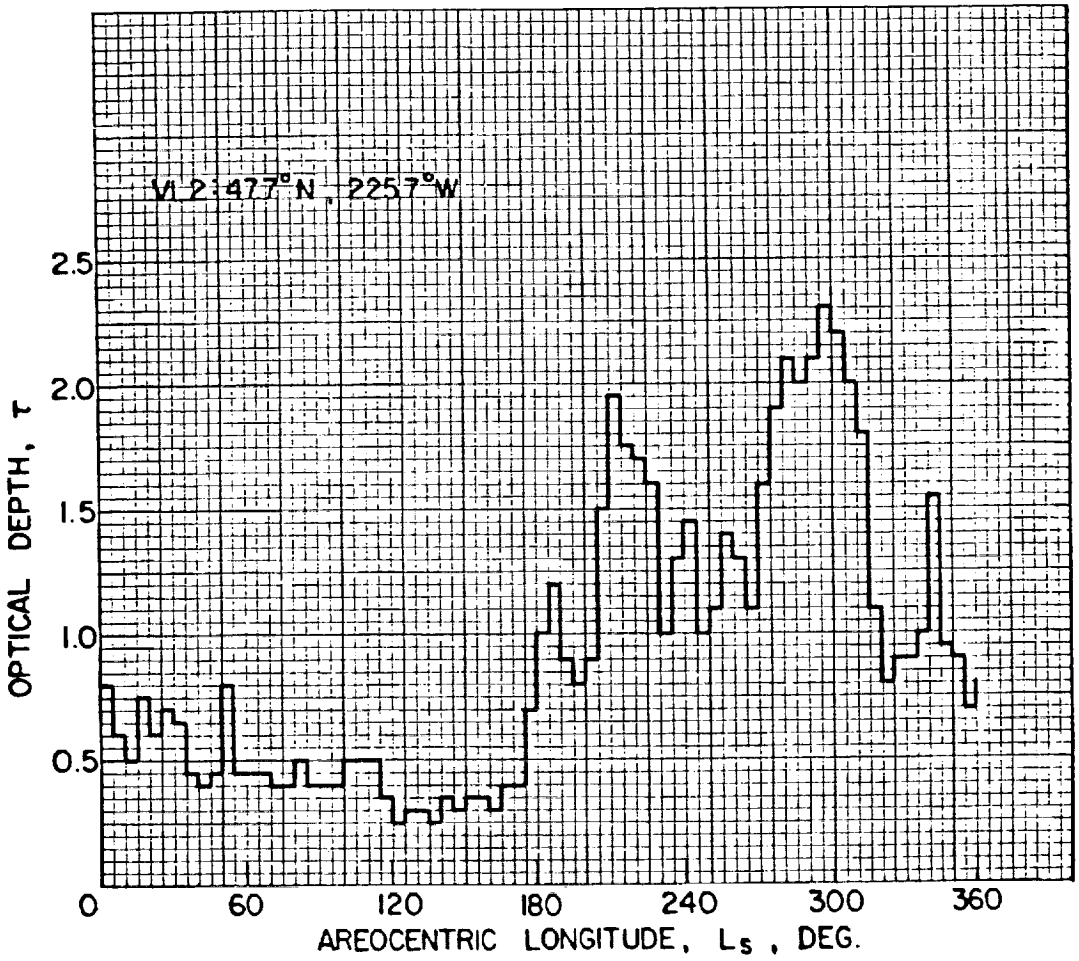

Fig. 2: Optical depth at Viking Lander VL2.

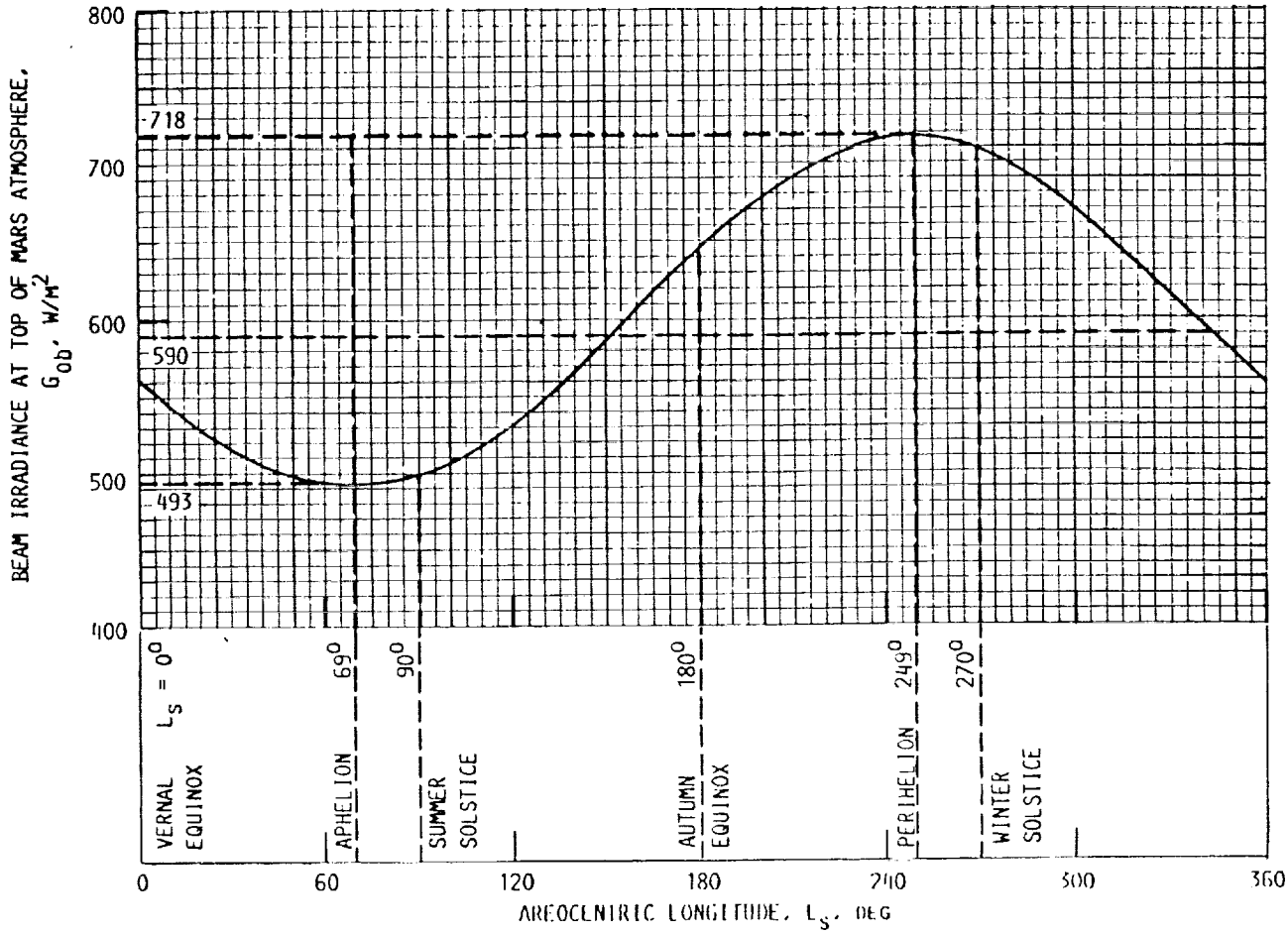

Fig. 3: Beam irradiance at the top of Mars atmosphere as function of areocentric longitude.

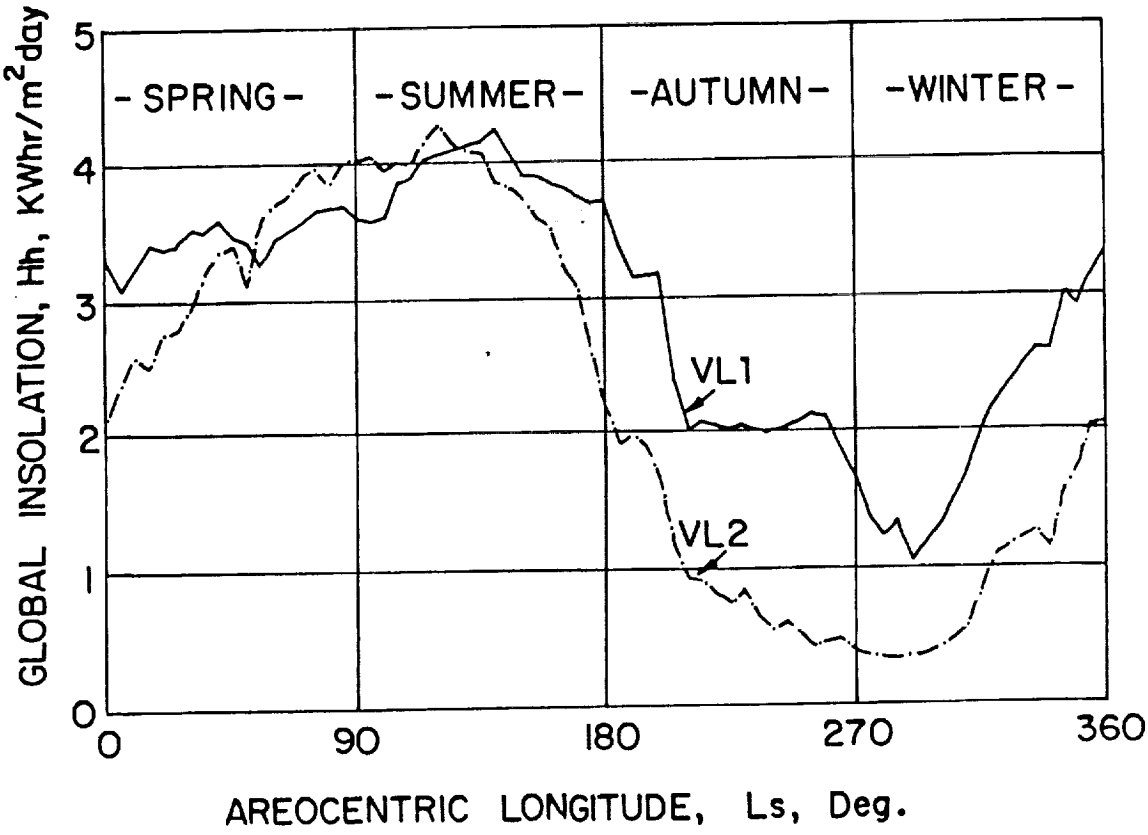

Fig. 4: Variation of daily global insolation H_h $(kWhr/m^2 - day)$ on a horizontal surface on Mars at VL1 and VL2 for a Martian year.

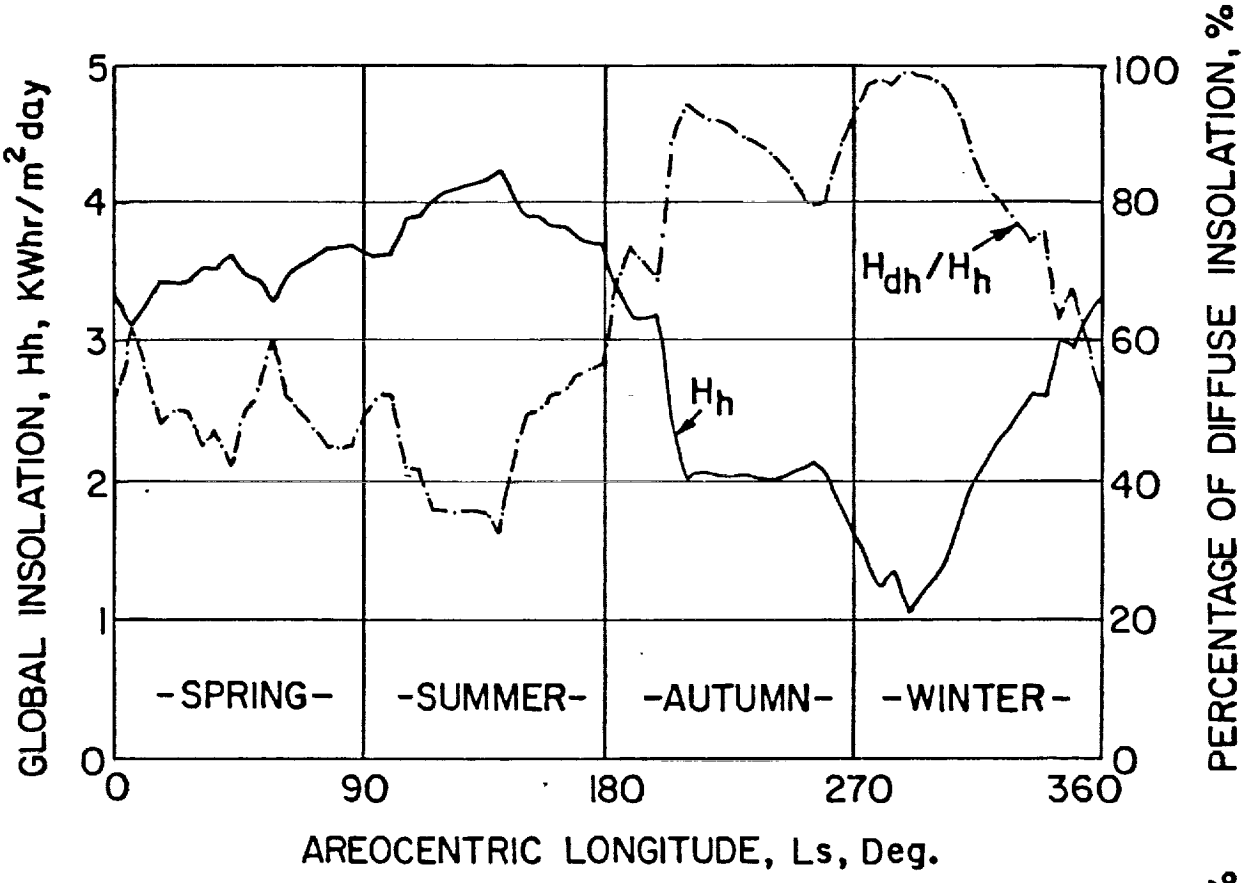

(a) VL1

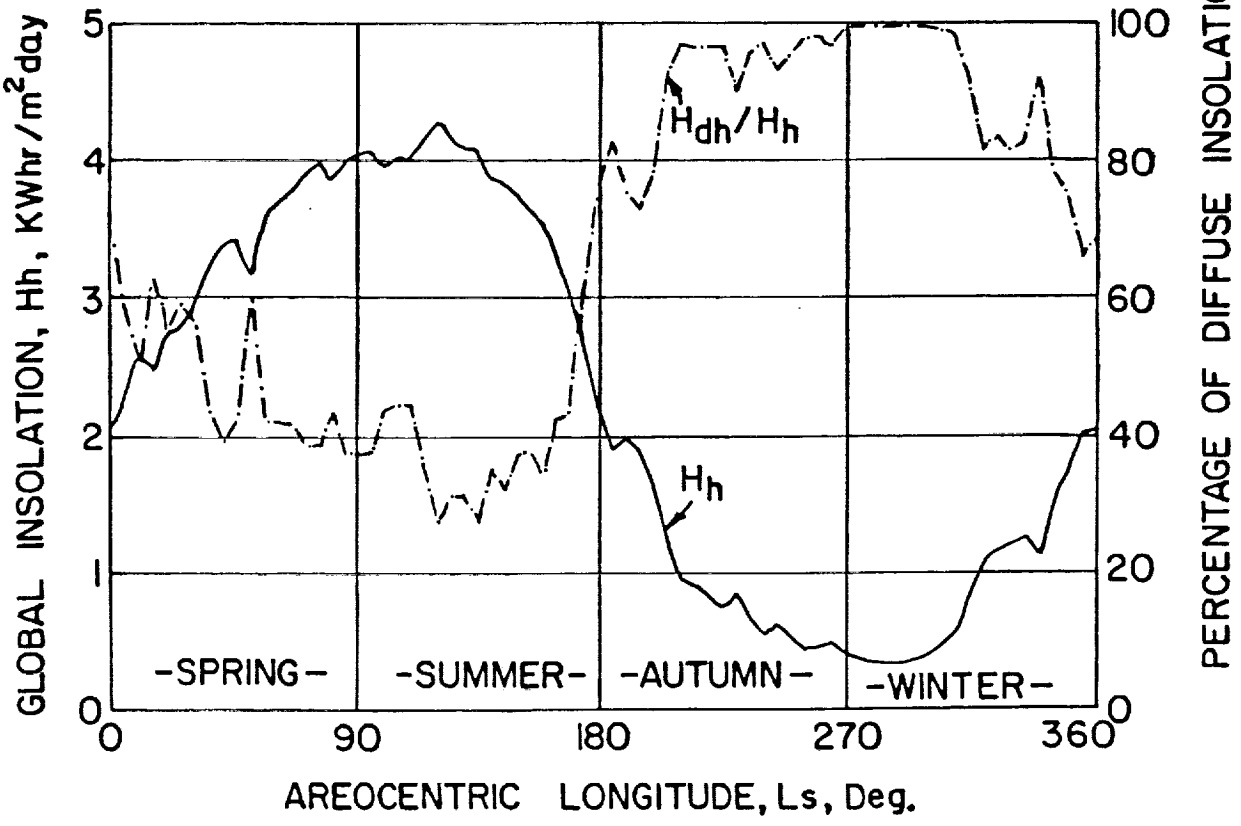

(b) VL2

Fig. 5: Variation of daily global insolation H_h $(kWhr/m^2 - day)$ and percentage of diffuse insolation H_{dh}/H_h on a horizontal surface on Mars at VL1 and VL2.

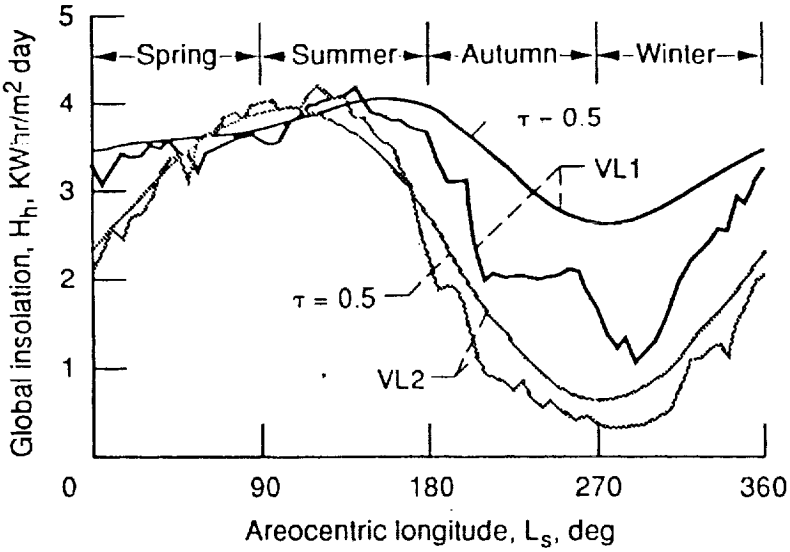

Fig. 6: Variation of daily global insolation H_h $(kWhr/m^2 - day)$ at VL1 and VL2 for the observed opacities at VL1 and VL2 and for $\tau = 0.5$.

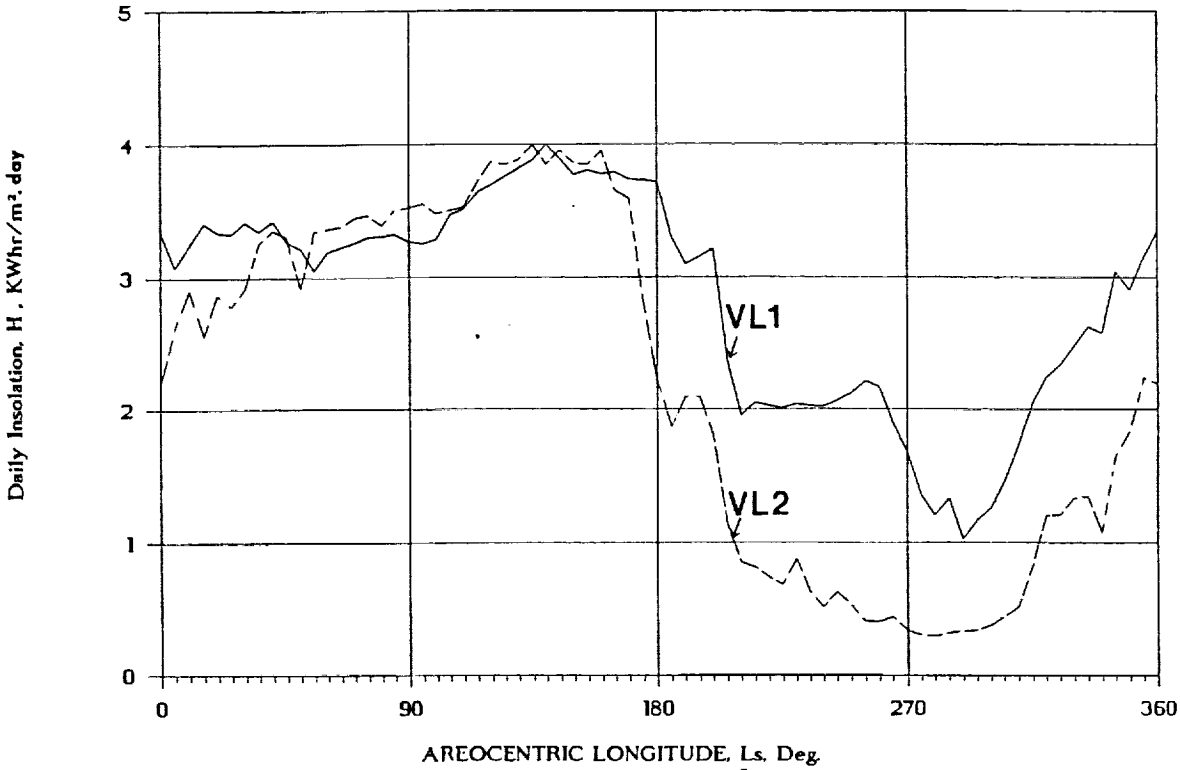

Fig. 7: Variation of daily global insolation H_β $(kWhr/m^2-day)$ on a tilted surface, $\beta = \phi$, at VL1 and VL2.

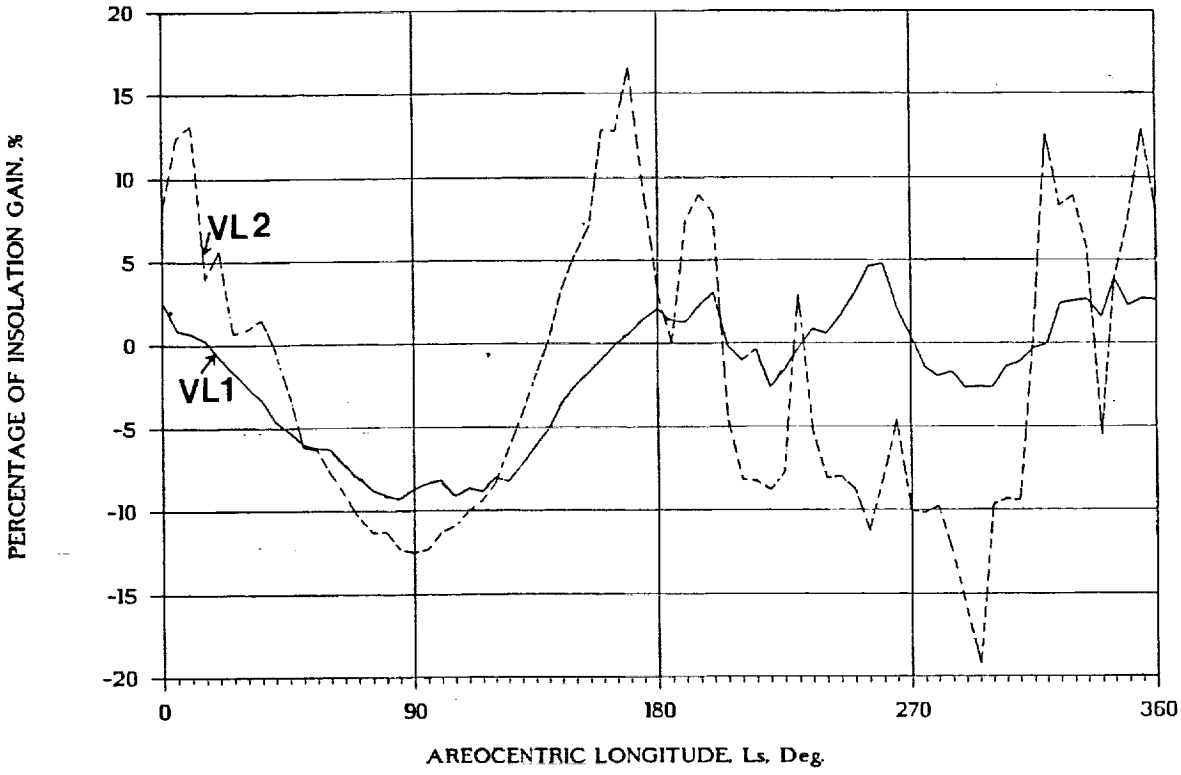

Fig. 8: Percentage of daily global insolation loss (gain) on a tilted surface $\beta = \phi$ as compared to a horizontal surface at VL1 and VL2.

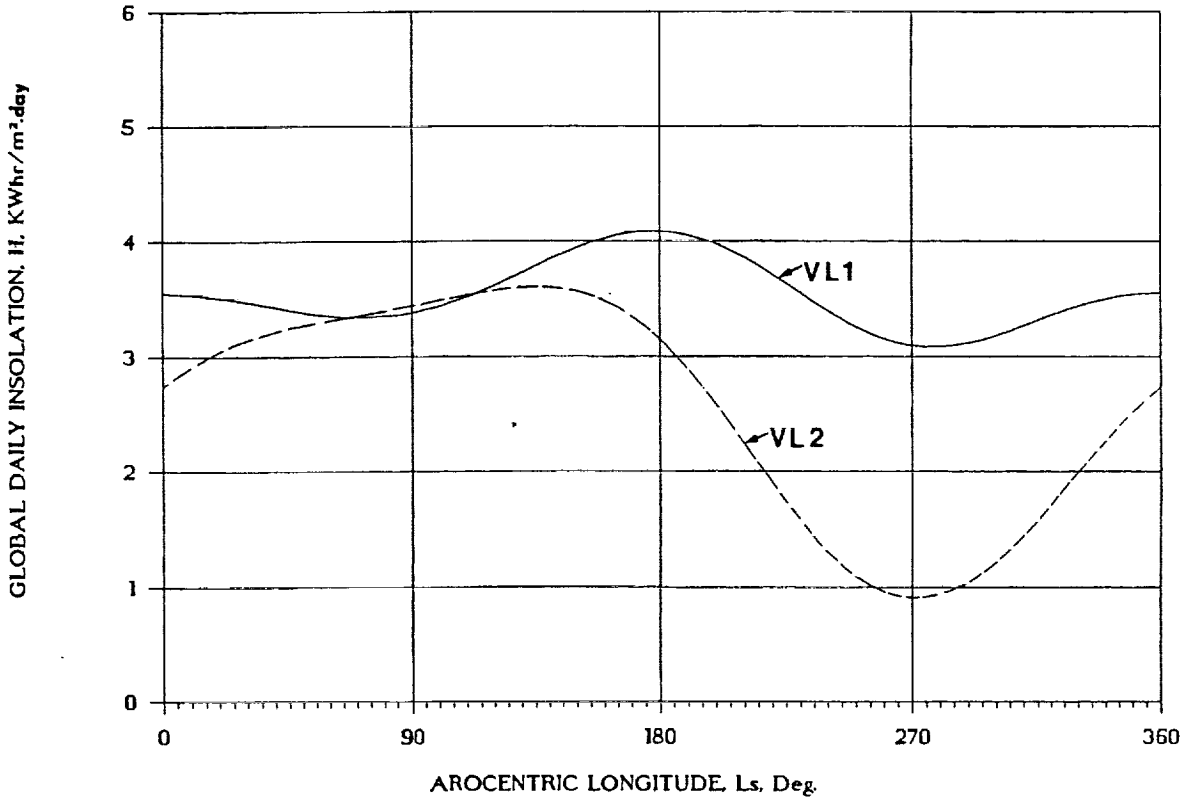

Fig. 9: Variation of daily global insolation H_β $(kWhr/m^2 - day)$ on a tilted surface, $\beta = \phi$, at VL1 and VL2 for $\tau = 0.5$.

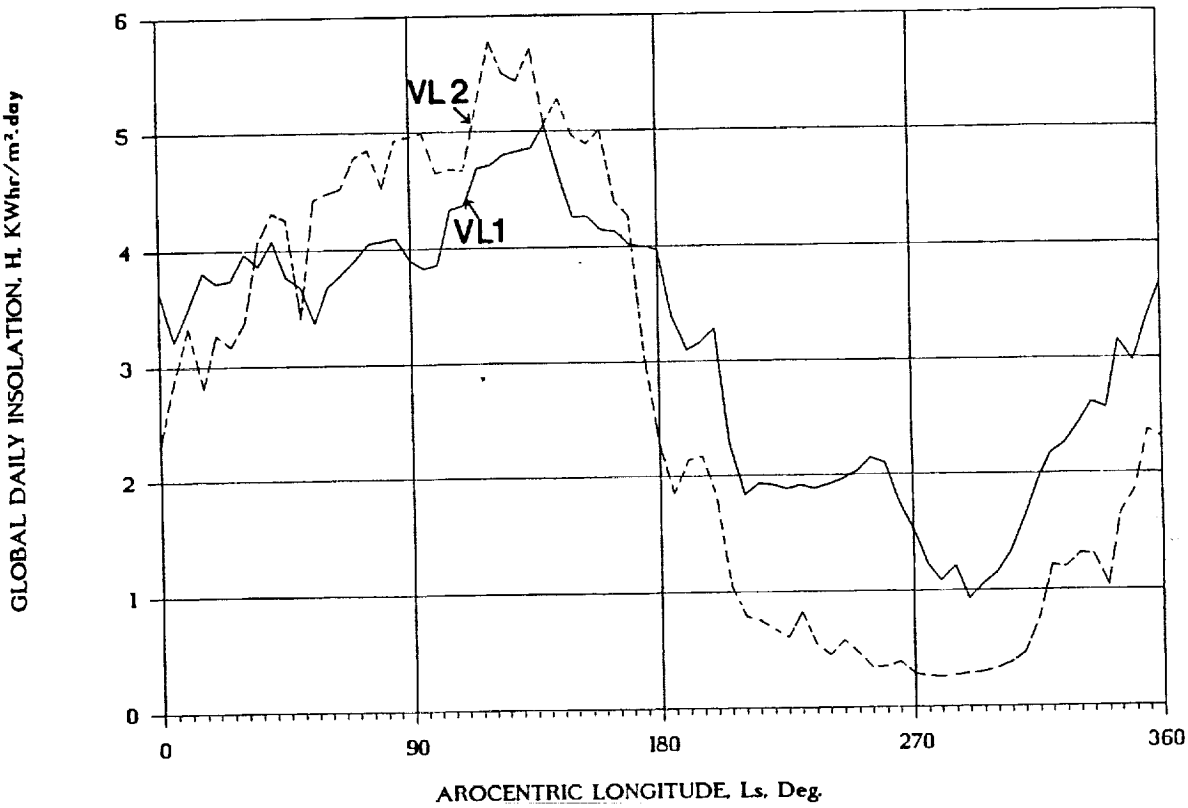

Fig. 10: Variation of daily global insolation H_{2x} $(kWhr/m^2 - day)$ on a two axis tracking surface at VL1 and VL2 for the observed opacities.

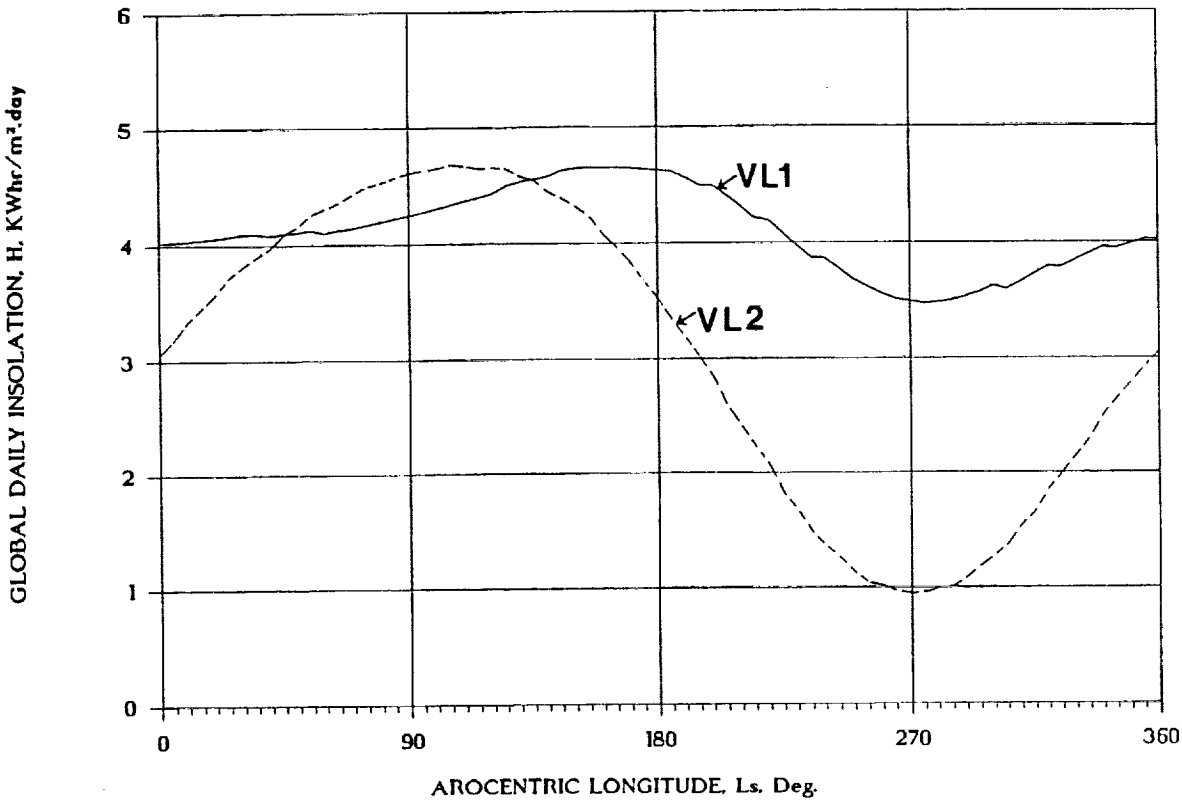

Fig. 11: Variation of daily global insolation H_{2x} $(kWhr/m^2 - day)$ on a two axis tracking surface at VL1 and VL2 for $\tau = 0.5$.

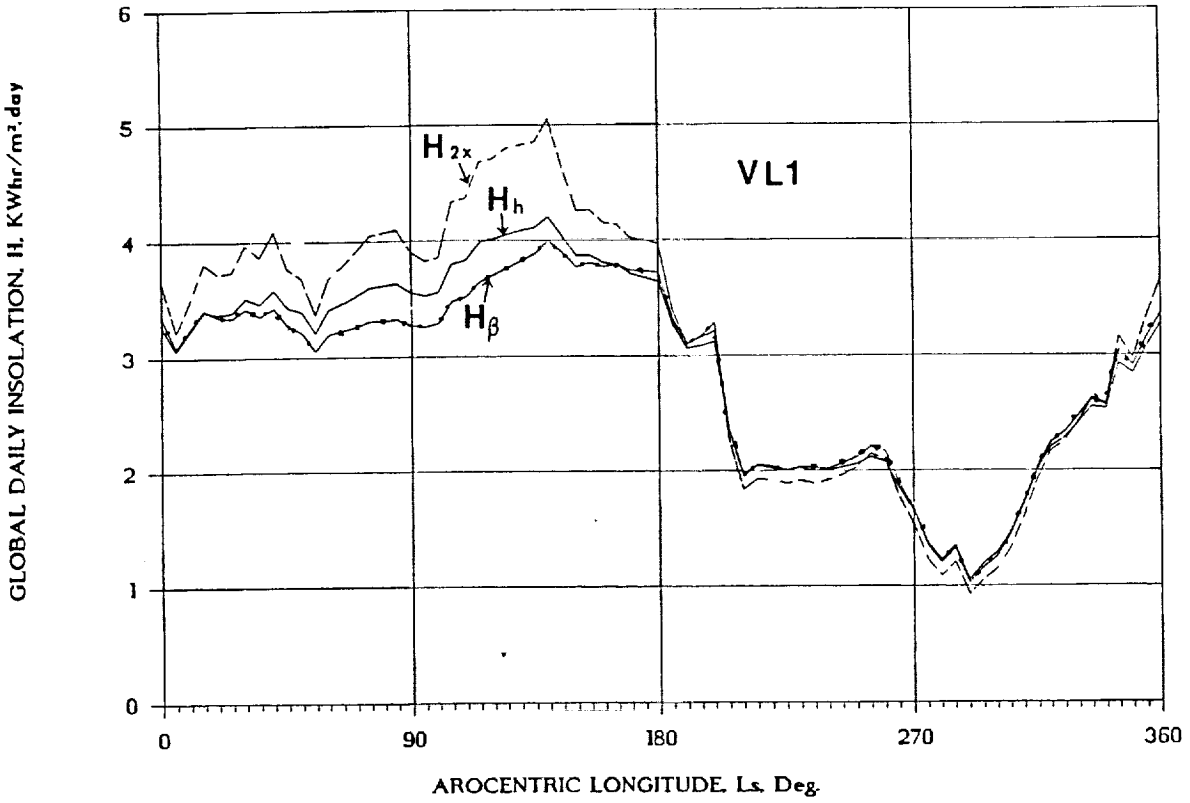

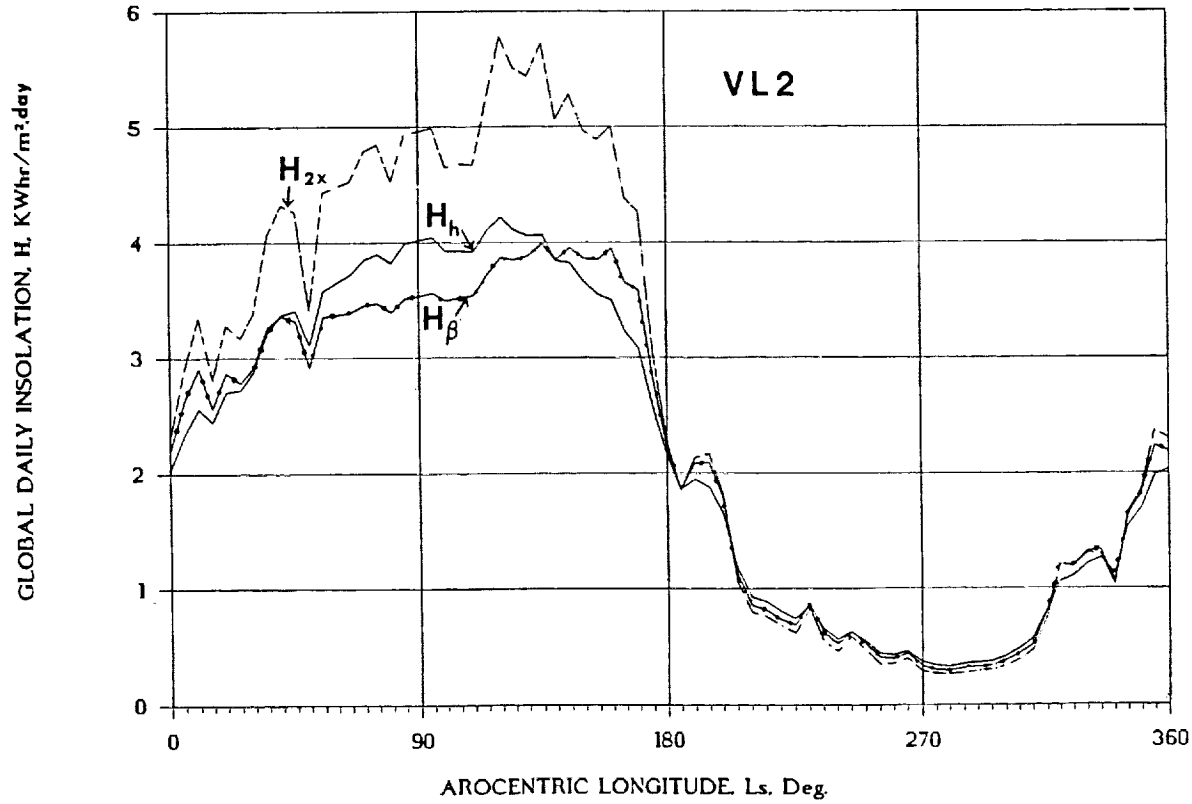

Fig. 12: Variation of daily global insolation H ($kWhr/m^2 - day$) on a horizontal surface H_h, inclined surface $H_\beta, \beta = \phi$; and on a two axis tracking surface H_{2x} for the observed opacities at VL1 and VL2.

REPORT DOCUMENTATION PAGE

Form Approved
OMB No. 0704-0188

Public reporting burden for this collection of information is estimated to average 1 hour per response, including the time for reviewing instructions, searching existing data sources, gathering and maintaining the data needed, and completing and reviewing the collection of information. Send comments regarding this burden estimate or any other aspect of this collection of information, including suggestions for reducing this burden, to Washington Headquarters Services, Directorate for information Operations and Reports, 1215 Jefferson Davis Highway, Suite 1204, Arlington, VA 22202-4302, and to the Office of Management and Budget, Paperwork Reduction Project (0704-0188), Washington, DC 20503.

1. AGENCY USE ONLY (*Leave blank*)	2. REPORT DATE	3. REPORT TYPE AND DATES COVERED
	August 1992	Technical Memorandum

4. TITLE AND SUBTITLE

Photovoltaic Array for Martian Surface Power

5. FUNDING NUMBERS

WU-506-41-11

6. AUTHOR(S)

J. Appelbaum and G.A. Landis

7. PERFORMING ORGANIZATION NAME(S) AND ADDRESS(ES)

National Aeronautics and Space Administration
Lewis Research Center
Cleveland, Ohio 44135-3191

8. PERFORMING ORGANIZATION REPORT NUMBER

E-7262

9. SPONSORING/MONITORING AGENCY NAMES(S) AND ADDRESS(ES)

National Aeronautics and Space Administration
Washington, D.C. 20546-0001

10. SPONSORING/MONITORING AGENCY REPORT NUMBER

NASA TM-105827

11. SUPPLEMENTARY NOTES

Prepared for the 43rd Congress of the International Astronautical Federation sponsored by the AIAA, NASA, and NAS, August 28-September 5, 1992. J. Appelbaum NASA Research Council-NASA Research Associate, on leave from Tel Aviv 69978 Israel (work funded by NASA Grant NAGW-2022). G.A. Landis, Sverdrup Technology, Inc., Lewis Research Center Group, 2001 Aerospace Parkway, Brook Park, Ohio 44142 (work funded by NASA Contract NAS3-25266). Responsible person, Geoffrey A. Landis (216) 433-2238.

12a. DISTRIBUTION/AVAILABILITY STATEMENT

Unclassified - Unlimited
Subject Category 92

12b. DISTRIBUTION CODE

13. ABSTRACT (*Maximum 200 words*)

Missions to Mars will require electric power. A leading candidate for providing power is solar power provided by photovoltaic arrays. To design such a power system, detailed information on solar radiation availability on the Martian surface is necessary. The variation of the solar radiation on the Martian surface is governed by three factors: (1) variation in Mars-Sun distance, (2) variation in solar zenith angle due to Martian season and time of day, and (3) dust in the Martian atmosphere. A major concern is the dust storms, which occur on both local and global scales. However, there is still appreciable diffuse sunlight available even at high opacity, so that solar array operation is still possible. Typical results for tracking solar collectors are also shown and compared to the fixed collectors. During the northern hemisphere spring and summer the isolation is relatively high, 2-5 kW-hr/m^2-day, due to the low optical depth of the Martian atmosphere. These seasons, totalling a full terrestrial year, are the likely ones during manned missions will be carried out.

14. SUBJECT TERMS

Mars; Optical thickness; Solar radiation; Global beam; Diffuse; Dust storm; Albedo; Solar cells

15. NUMBER OF PAGES

22

16. PRICE CODE

A03

17. SECURITY CLASSIFICATION OF REPORT	18. SECURITY CLASSIFICATION OF THIS PAGE	19. SECURITY CLASSIFICATION OF ABSTRACT	20. LIMITATION OF ABSTRACT
Unclassified	Unclassified	Unclassified	